

## Width of cluster plasmon resonances: Bulk dielectric functions and chemical interface damping

H. Hövel, S. Fritz, A. Hilger, and U. Kreibitz

*1. Physikalisches Institut der Rheinisch-Westfälischen Technischen Hochschule Aachen, 52056 Aachen, Federal Republic of Germany*

M. Vollmer

*Fachbereich Physik der Universität Kassel, 34132 Kassel, Federal Republic of Germany*

(Received 27 May 1993; revised manuscript received 10 September 1993)

The damping of collective electron resonances in clusters which develop into plasmon polaritons at larger sizes is investigated for free, supported, and embedded neutral metal clusters. Embedding of free 2 nm Ag clusters of 2-nm diameter into a SiO<sub>2</sub> matrix leads to an increase of the width of the resonances by more than a factor of 3. The optical spectra are compared with the Mie theory using size-effect-modified dielectric functions of the solid state. The results corroborate the assumption that the widths of the resonances strongly depend on chemical interface effects. The results are briefly discussed with regard to limited-mean-free-path and quantum-size-effect theories and a recent approach by Persson. It is demonstrated that the widths of the spectra of supported and embedded clusters have to be interpreted with care since true intrinsic size effects of the clusters appear to be less effective than previously believed and can be obscured by the chemical interface damping.

### I. INTRODUCTION

Collective electron resonances induced by electromagnetic radiation in neutral metal clusters (Mie resonances) and denoted as plasmon polaritons in the limit of large size have already been investigated for many decades. Recently, however, there has been a revival in interest which is reflected in an increased number of experiments. This is due to development of metal-cluster-beam technology which allows experiments on free clusters rather than merely on supported or embedded clusters. In addition to the classical extinction/absorption spectroscopy the optical spectra of free metal clusters can also be studied with beam depletion spectroscopy.

### II. THEORETICAL APPROACHES

*Ab initio* quantum theoretical approaches<sup>1</sup> give adequate descriptions of the spectral positions of the resonances for the very small clusters (number of atoms  $N \leq 8$ ) and are presently being extended to larger sizes. Alternatively, large clusters are treated within the jellium model, which also yields multiple line structures in the spectra, part of which are interpreted as collective electron resonances.<sup>2</sup> Both kinds of theories provide peak positions, but have problems predicting peak shapes or widths. This drawback is overcome by a third approach, the Mie theory, based on the solid state which applies classical electrodynamics to clusters of simple shapes like spheres. The resulting Mie resonances cause selective optical extinction bands in the visible spectral range for the alkali and noble metals, which usually depend strongly on the cluster diameter  $2R$ . For large sizes they are interpreted as spherical plasmon polaritons whereas in small clusters they are referred to as collective electron excitations.<sup>3,4</sup>

This distinction is motivated by the hot-electron effect.

In large clusters or bulk metals, plasmonlike excitations are based upon almost elastic processes for the involved electrons due to the field-induced coherent oscillation superimposed on their  $\mathbf{k}$  vectors. The individual electrons gain only small amounts of energy of the order  $\Delta E \approx \hbar\omega/N_e$ , where  $\hbar\omega$  is the excitation energy and  $N_e$  is the number of participating electrons in the cluster. In contrast, this energy becomes important in small clusters ( $\Delta E \approx 0.1$  eV for  $N_e \approx 100$ ) and hot electrons are produced. The smaller the cluster, the hotter the electrons will be, and in such a case we prefer not to denote the excitation as a plasmon but rather speak of collective electron excitation.

From semiconductors it is well known that hot electrons suffer intense electron-electron scattering because of the softening of the Fermi surface. The probability of these scattering events is proportional to  $(\Delta E)^2$  and phase coherences are strongly disturbed. In bulk metals such effects are less important, but in small clusters this may no longer be true because of larger  $\Delta E$  values. Hence, this might be an additional size-dependent effect destroying the phase coherence, on which the collective resonances are based.

Among the above three approaches the Mie theory has advantages of being conceptually simple by treating the electromagnetic fields separately from the linear-response properties of the cluster material—which are introduced by phenomenological data—and of also providing bandwidths. Keeping the problems of other theories concerning the plasmon damping in mind it appears promising to extend the Mie theory calculations also to very small metal clusters. In this paper we focus on the plasmon polariton width and will demonstrate that caution is advisable along the way. First, results strongly depend on the choice of the size-dependent optical material functions used in the computations. In this paper we will focus on a second aspect, namely that chemical interface effects

can have drastic influences on the spectra far beyond the small ones already included in the frame of Mie's theory.

### III. SIZE DEPENDENCE OF OPTICAL MATERIAL FUNCTIONS

#### A. Free-electron metals

In the following we briefly describe the predictions of the Mie theory for metal clusters that show cluster-size effects in the optical spectra. This leads to theoretical models for the size dependencies of the dielectric functions and the definition of a relevant parameter which can be compared to experiment.

Below characteristic sizes (15 nm for Ag, 25 nm for Au, etc.) the electrodynamic effect of the local-field enhancement, described by the Mie theory, becomes independent of  $R$ . In this case ( $2R \ll \lambda$ ), retardation effects that lead to radiative plasmon damping disappear and the extinction cross section is given by dipole absorption, only

$$\sigma_{\text{abs}}(\omega) = 9 \frac{\omega}{c} \varepsilon_m^{3/2} V_0 \frac{\varepsilon_2(\omega)}{[\varepsilon_1(\omega) + 2\varepsilon_m]^2 + \varepsilon_2(\omega)^2} \quad (1)$$

$V_0$  is the spherical particle volume and  $\varepsilon_m$  and  $\varepsilon(\omega) = \varepsilon_1(\omega) + i\varepsilon_2(\omega)$  denote the dielectric functions of the surrounding medium and of the particle material, respectively. The cluster properties are thus attributed to the material properties of the bulk solid.

This cross section has a narrow resonance whose position  $\omega_1$  and shape is governed merely by the dielectric functions. The dipole resonance frequency is determined by the condition  $\varepsilon_1(\omega) = -2\varepsilon_m$  provided  $\varepsilon_2(\omega)$  is not too large and does not vary much in the vicinity of the resonance.

Within the Drude-Lorentz-Sommerfeld free-electron model  $\varepsilon(\omega)$  is given by

$$\varepsilon(\omega) = 1 - \frac{\omega_p^2}{\omega^2 + i\gamma\omega} \quad (2)$$

where the plasma frequency  $\omega_p = (ne^2/\varepsilon_0 m_{\text{eff}})$  depends on the electron density  $n$  and on the proper electron effective mass  $m_{\text{eff}}$ . Using Eq. (2) and the condition  $\omega \approx \omega_1$  we can rewrite Eq. (1) in terms of a simple Lorentzian, the full width at half maximum being given by the phenomenological damping constant  $\gamma$ .

$$\sigma_{\text{abs}}(\omega) = \sigma_0 \frac{1}{(\omega - \omega_1)^2 + \left[\frac{\gamma}{2}\right]^2} \quad (3)$$

with  $\omega_1$  being the frequency of the (undamped) Mie resonance  $\omega_1 = \omega_p / \sqrt{1 + 2\varepsilon_m}$ . It should be pointed out that the Drude  $\gamma$  of Eq. (2) equals the bandwidth of the dipole plasmon polariton in Eq. (3) for the case of free electrons. This is a peculiarity for free-electron metals and does not hold for realistic metals (see below).

In the classical theory of free-electron metals, the damping is due to the scattering of the electrons with phonons, electrons, lattice defects, or impurities. The re-

lation  $\gamma = v_F / l_\infty$  holds where  $v_F$  is the Fermi velocity and  $l_\infty$  the mean free path of the electrons in bulk material, given by Matthiessen's rule (see, e.g., Ref. 5).

In Eq. (1) the cluster size is directly enclosed only in the prefactor  $V_0$ , which does not influence the resonance position or shape. In experiments on cluster-matrix systems, however, one observes a dramatic increase of the Mie bandwidth and usually small peak shift of the resonance for decreasing cluster size. While for the peak shifts there is still a controversy even concerning the direction of the shift<sup>6-9</sup>, there is unequivocal experimental evidence that in systems with weak cluster-matrix interactions, the width follows a well-established size dependence.<sup>6,9,10</sup> In particular, several experimental data were well fitted with the following relation for the full width at half maximum  $\Gamma_{\text{expt.}}(R)$  over wide size ranges between 2 and 20 nm diameter:

$$\Gamma_{\text{expt.}}(R) = \Gamma_0 + a/R \quad (4)$$

where  $a$  is the slope constant of the size dependence and  $\Gamma_0$  is size independent. As just pointed out, Eq. (4) is in sharp contrast to Eq. (1) which predicts size independent electromagnetic response when using bulk dielectric functions. Consequently such size effects are exclusively due to size effects of the cluster material including the cluster surface/interface. Still, the Mie theory formula [Eq. (1)] is a good description if a dielectric function  $\varepsilon(\omega, R)$  is used which varies properly as a function of particle size. This ( $1/R$ ) law and its temperature dependence were established and correlated to corresponding dielectric functions in Refs. 7 and 11.

We want to point out once more the conceptual difference between the Drude damping constant  $\gamma$  and the width  $\Gamma$  of the Mie resonances and again note that only for the free-electron metals treated in this section do the two equal each other.

The classical *free path effect* model argues that if the cluster sizes become comparable with  $l_\infty$  the interactions of the conduction electrons with the particle surface become important as an additional collision process resulting in a reduced effective mean free path  $l$  and increased  $\gamma$  which now depends on cluster size

$$\gamma(R) = \gamma_0 + (A v_F)/R \quad (5)$$

where  $A$  includes details of the scattering processes.<sup>7,12</sup>

A number of quantum theoretical approaches has been developed to compute the width  $\Gamma$ . Depending on the level of approximation the size-dependent polarizability  $\alpha(\omega, R)$  or equivalently the dielectric function  $\varepsilon(\omega, R)$  of the cluster material are regarded as composed of locally varying or nonlocal contributions, or as averaged over the cluster volume, including the surface/interface. The common feature of such theories is that they deal with the confinement of the cluster.<sup>8,10</sup> However, recent work concentrates on the deciding importance of the confining surface/interface itself.<sup>12,13</sup>

In most models concerning free-electron metals the size dependence of the bandwidth is usually expressed as

$$\Gamma_{\text{theor.}}(R) = \Gamma_\infty + (A^* v_F)/R \quad (6)$$

where  $A^*$  is a theory-dependent constant of the order of 1. A compilation of  $A^*$  values was given in Ref. 6. Replacing the Drude constant  $\gamma$  in the dielectric function  $\epsilon(\omega)$  of Eq. (2) by  $\Gamma_{\text{theor}}(R)$  in turn gives an appropriate size-dependent  $\epsilon(\omega, R)$  for the special case of free-electron metal clusters.

### B. Realistic metals

In realistic metals, interband transitions alter the simple form of  $\epsilon(\omega)$  for free electrons and in most metals they are important in the spectral region of Mie resonances. Examples for such *worse free-electron metals* are Au, Cu, or Li, but also Ag clusters which have a Mie bandwidth smaller than the corresponding one for free-electron clusters. As a rule of thumb, the peak position and width of the Mie band of good free-electron metals are essentially determined by  $\epsilon_1(\omega)$  and  $\epsilon_2(\omega)$  with  $\epsilon_1(\omega_1) = -2\epsilon_m$  and  $\Gamma = \gamma$ , respectively. Realistic metals require a more elaborate theoretical model for the bulk  $\epsilon(\omega)$  and they usually show additional influence of the spectrum of  $\epsilon_1(\omega)$  onto the size-dependent width and vice versa of  $\epsilon_2(\omega)$  on the position of the resonance.

In general, the influence of  $\epsilon(\omega)$  on the Mie resonances can lead to quite complex spectra. Figure 1 shows the absorption cross section calculated with Eq. (1) as a function of frequency for four different pairs of hypothetical dielectric functions. It demonstrates that  $\epsilon_1(\omega)$  determines peak positions and also influences the widths. Steep  $\epsilon_1(\omega)$  spectra yield narrow resonances [Fig. 1(a)] whereas flat  $\epsilon_1(\omega)$  spectra give broad absorption bands for the same  $\epsilon_2$  [Fig. 1(b)]. Figure 1(c) proves that in princi-

ple multipeak structures can be produced by appropriate  $\epsilon_1(\omega)$  spectra. However, they may easily be damped away if  $\epsilon_2(\omega)$  is sufficiently large as shown in Fig. 1(d), where  $\epsilon_1(\omega)$  is identical to Fig. 1(c), but two of the three resulting peaks in Fig. 1(c) have vanished due to larger  $\epsilon_2(\omega)$ . This figure exemplifies that low  $d\epsilon_1(\omega)/d\omega$  and large  $\epsilon_2(\omega)$  tend to smear out the resonances, sometimes past recognition. In practice only a few materials, like the alkali and noble metals as well as aluminum, exhibit sharp resonances.

From a general point of view, it would be best to calculate the polarizability  $\alpha(\omega, R)$  or the dielectric function  $\epsilon(\omega, R)$  from first principles,<sup>2</sup> i.e., from the size-dependent electron-energy-level scheme. This, however, proves difficult even for moderately large clusters.

In a semiclassical extension of the Drude formula [Eq. (2)] for realistic metals the linear-optical response regarding all relevant electronic transitions is traced back to the band-structure model of the solid state. The resulting dielectric function is now not only determined by the Drude quantities—electron density  $n$ , effective electron mass  $m_{\text{eff}}$ , and  $\gamma$  of Eq. (2)—but also by band-structure  $E(\mathbf{k})$  and transition matrix elements  $\mathbf{e} \cdot \mathbf{M}_{fi}(\mathbf{k})$ , describing interband transitions between initial ( $i$ ) and final ( $f$ ) states, with  $\mathbf{e}$  the polarization vector in the direction of the electric field. A basic expression was given by Bassani and Parravicini:<sup>14</sup>

$$\epsilon(\omega) = 1 - \frac{(ne^2/\epsilon_0 m_{\text{eff}})}{\omega^2 + i\gamma\omega} + \chi^{\text{inter}} \quad (7)$$

with

$$\chi^{\text{inter}} = \frac{8\hbar^3 \pi e^2}{m^2} \sum_{i,f} \int_{\text{BZ}} \frac{2d\mathbf{k}}{(2\pi)^3} |\mathbf{e} \cdot \mathbf{M}_{fi}(\mathbf{k})|^2 \left\{ \frac{1}{[E_f(\mathbf{k}) - E_i(\mathbf{k})][|E_f(\mathbf{k}) - E_i(\mathbf{k})|^2 - \hbar^2 \omega^2]} + i \frac{\pi}{2\hbar^3 \omega^2} \delta[E_f(\mathbf{k}) - E_i(\mathbf{k}) - \hbar\omega] \right\}.$$

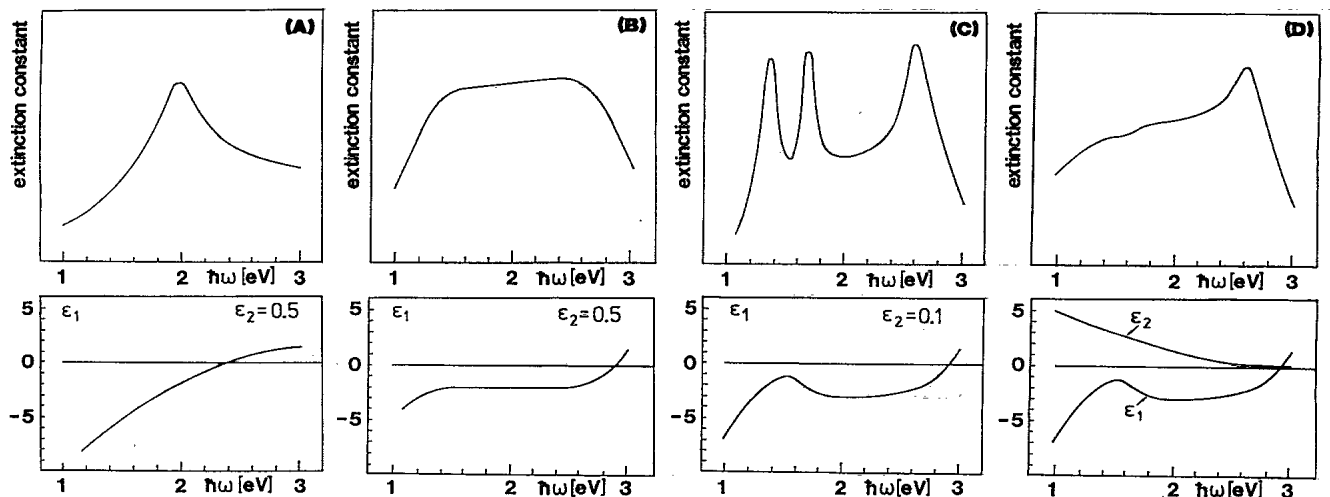


FIG. 1. Model calculations of Mie extinction spectra ( $2R = 10$  nm,  $\epsilon_m = 1$ ) demonstrating the influences of the dielectric material function  $\epsilon(\omega) = \epsilon_1(\omega) + i\epsilon_2(\omega)$ . Details: see text.

In principle, all quantities  $n$ ,  $m_{\text{eff}}$ ,  $\gamma$ ,  $E_i(\mathbf{k})$ ,  $E_f(\mathbf{k})$ , and  $\mathbf{M}_{fi}(\mathbf{k})$  will develop size dependencies for sufficiently decreased cluster size. For example, local changes of the material properties like electron density, atomic distances, etc. close to the cluster surface (which is smooth to different extents for the  $s$  electrons, energetically deeper lying electrons, and for the ion cores) do affect  $\varepsilon(\omega)$ . Because of the increasing importance of the surface towards smaller cluster sizes,  $\varepsilon(\omega)$  then develops additional size dependencies. However, the free path effect of Eq. (5) usually exceeds all of these by far, being probably the strongest of all known cluster-size effects also for realistic metals.

In the framework of the Mie theory the appropriate  $\varepsilon(\omega, R)$  is regarded as the very cluster averaged quantity (the average conveniently including the surface or interface) which—inserted into the theory—quantitatively reproduces the measured absorption or extinction spectra. Vice versa,  $\varepsilon(\omega, R)$  and hence the coefficient  $A$  can be extracted from experimental data as was performed for Ag and Au clusters by a Kramers-Kronig analysis.<sup>7,11</sup> These  $\varepsilon(\omega, R)$ , shown in Fig. 2 for the case of Ag clusters at room temperature, were compared to the optical properties of the bulk metal. The size effects proved to decrease monotonously both for  $\varepsilon_1$  and  $\varepsilon_2$  in the limit  $(1/R) \rightarrow 0$  and quantitative correspondence with the bulk dielectric function was obtained in this limit as is also shown in Fig. 2 (left-hand side). These evaluations were later extended to determine in addition also the temperature dependence of  $\varepsilon(\omega, R)$ .<sup>7</sup>

Such a determination of the dielectric function of bulk material by extrapolating formally to  $(1/R) \rightarrow 0$  has the advantage of being free of difficulties due to large scale nonlocalities like the anomalous skin effect (which, yet, is absent for most metals in the visible region).

In detail, the size correction of literature values  $\varepsilon_{\text{bulk}}(\omega)$  in the right-hand side graphs of Fig. 2 was performed by replacing the bulk Drude term of Eq. (7) with the size-dependent one depending on  $\gamma(R)$  of Eq. (5):

$$\varepsilon(\omega, R) = \varepsilon_{\text{bulk}}(\omega) + \frac{\omega_p^2}{\omega^2 + i\omega\gamma_0} - \frac{\omega_p^2}{\omega^2 + i\omega(\gamma_0 + A\nu_F/R)} \quad (8)$$

In summary the almost quantitative correspondence of experimental and calculated  $\varepsilon(\omega, R)$  spectra, as well as the convergence toward the bulk literature values, confirm the use of bulk dielectric functions corrected by Eq. (5) to explain the optical properties of such clusters down to at least  $N = 2 \times 10^2$  atoms per cluster in the spectral region of the Mie resonance. In this range the interband transitions do not strongly contribute in Ag clusters and, hence, will not be treated further in this paper. This is peculiar for Ag since from analogous investigations on Au clusters it is well known that already below about  $N = 5 \times 10^2$  the interband contributions drastically change with size.<sup>15</sup> Additional size effects in the  $s$  electrons beyond Eq. (5) which very probably occur in  $n$  and  $m_{\text{eff}}$  are smaller than the dominating  $(1/R)$  effect and were not identified.

In order to find a direct relation between experimental

widths of the resonances and theoretical size-effect parameters, i.e., between parameters  $a$  and  $A$  of formulas (4) and (5) for the case of realistic dielectric functions, we start with Taylor expansions for  $\varepsilon_1(\omega)$  and  $\varepsilon_2(\omega)$  around the resonance frequency  $\omega_1$ , and insert them into Eq. (1). This results in (see Ref. 16)

$$\Gamma_{\text{theor}}(R) = \frac{2\varepsilon_2(\omega_1, \gamma(R))}{\left[ \left[ \frac{d\varepsilon_1(\omega)}{d\omega} \Big|_{\omega_1} \right]^2 + \left[ \frac{d\varepsilon_2(\omega)}{d\omega} \Big|_{\omega_1} \right]^2 \right]^{1/2}} (1 + \eta) \quad (9)$$

Usually  $\eta \ll 1$  holds for good metals. For Ag (but not for Au) we can simplify Eq. (9) because  $(d\varepsilon_1/d\omega)^2 \gg (d\varepsilon_2/d\omega)^2$ . Inserting  $\varepsilon_2$  with  $\gamma(R)$  of Eq. (5) finally gives

$$a \approx \frac{2\omega_p^2}{\omega^3} \frac{\nu_F}{|d\varepsilon_1/d\omega|} A \quad (10)$$

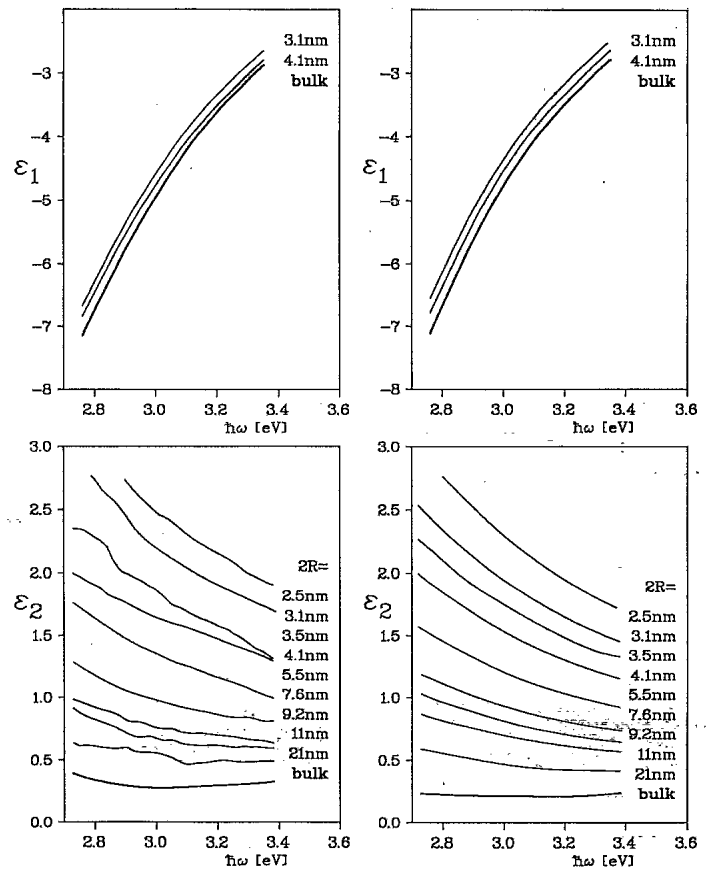


FIG. 2. Dielectric material functions  $\varepsilon_1(\omega, R)$  and  $\varepsilon_2(\omega, R)$  of Ag clusters embedded in glass, determined by the Kramers-Kronig analysis of measured absorption spectra (left). They are compared to results obtained from  $\varepsilon(\omega)$  of bulk Ag; size corrected by Eq. (8) with  $A = 1$  (right) (after Ref. 11). The bulk spectra of the graphs on the left-hand side were obtained by extrapolating the experimental values to  $(1/R) \rightarrow 0$ . The bulk spectra in the right-hand graphs are the literature values.

In general  $\varepsilon_1$  and  $d\varepsilon_1/d\omega$  also depend on  $R$  as follows from Eqs. (7) and (8). Equation (10) allows us to compare experimental slope constants  $a$  derived from Eq. (4) with theoretical size-effect parameters  $A$  and  $A^*$  [Eqs. (5) and (6)].

#### IV. SURVEY OF EXPERIMENTAL RESULTS

Most optical experiments with clusters were performed with clusters either on supports or embedded in liquid or solid surrounding matrices. Hence, quantitative tests of the  $\Gamma(R)$  dependence were up to now limited to complex cluster-matter systems containing besides the clusters also embedding or substrate materials. Few experiments<sup>17,18</sup> were performed on clusters produced by high-pressure gas aggregation as smoke<sup>19</sup> and on a free Hg cluster beam,<sup>20</sup> however, no  $\Gamma(R)$  dependencies were evaluated for these systems. Recently depletion spectra of ionized, mass selected, free Hg clusters were evaluated applying Eq. (6), and  $A \approx 0.4$  was obtained.<sup>21</sup>

We now turn to neutral Ag clusters. Figure 3 compiles experimentally determined widths for the example of differently embedded Ag clusters with sizes small enough such that Eq. (1) holds. In this plot, we adopt the common practice of measuring  $\Gamma$  in eV, i.e., we plot  $\hbar\Gamma$  rather than  $\Gamma$ . The data can be divided into two groups.

(1) Systems which clearly follow the  $(1/R)$  size dependence [Eq. (4)], yet with slope parameters depending on the surrounding material. Characteristic for these samples is that the matrices are only weakly interacting with the clusters (e.g., solid rare gases or glass). The constants  $\Gamma_0$  extracted from the experimental data agree quite well with theoretical predictions from bulklike linear response.

(2) Systems with strongly increased damping but without any clear correlation to the cluster size. The

constants  $\Gamma_0$  extracted from these data lead to discrepancies from 0.2 to 0.7 eV when compared to theories. These samples are characterized by high ionicity of the matrix. The reason for the absence of a clear size dependence as obvious in the series, denoted by  $\blacktriangledown$ ,  $\triangle$ ,  $\square$ , and  $\blacksquare$  in Fig. 3 is unknown. Scattering at interior defects, included impurities, or chemical reactions at the interface are possibly responsible.

In liquid colloidal solutions chemical reactions including charge transfer to or from the clusters have proven to change  $\Gamma$  strikingly as is evident from the two examples of reactions with OH radicals and with iodine, also plotted in Fig. 3. This behavior has been used to identify chemical reactions in the electrolyte.<sup>22,23</sup>

In the following we shall exclusively focus on Ag cluster systems which obey the  $1/R$  law and disregard samples of the second type. The results of Charlé, Frank, and Schulze,<sup>9</sup> indicated in Fig. 3 by the interpolation lines of their data points, allow a straightforward classification of the chemical influence of the surrounding medium by the width parameter  $A$ . It is strongest for non-noble solid gases like CO ( $A=0.9$ ) and drops for solid rare gases from Ar to Ne ( $A=0.26$ ). High-temperature matrices like glass yielded  $A=1$  [a similar system of Au clusters even gave a value of  $A=1.4$  (Ref. 11)].

Up to now the interpretation of the various values of  $A$  as being caused by the chemical composition of the interface still suffered from one missing link, namely the measurement of the absorption spectrum of adsorbate-free and noninteracting neutral Ag clusters of comparable size. This gap has now been closed by our experiments and we present such spectra in the following.

#### V. OPTICAL SPECTRA OF FREE, SUPPORTED, AND EMBEDDED CLUSTERS

##### A. Experimental setup

A high-temperature nozzle source produces silver clusters in a supersonic expansion. The source, a heated skimmer, and a cooled beam collimator (15 K) were optimized to produce a high intensity cluster beam with mean sizes  $2R$  of about 2 nm ( $N \approx 300$  atoms/cluster) and narrow-size distribution. No additional size selection was carried out. The source was heated to 2300 K and the expansion through the conical nozzle was performed using Ar of about 5 bars stagnation pressure as carrier gas. The source parameters were chosen similar to those found by Hagen<sup>24</sup> who by mass spectroscopy proved them to be optimal for the production of Ag clusters. Beam densities correspond to a deposition rate of 230 nm/s in a distance of 0.3 m from the nozzle. The gas-dynamic velocity amounts to  $\approx 1.5 \times 10^3$  m/s. The beam diverges to a diameter of 30 mm in a distance of 1 m from the nozzle. Fast optical extinction measurements were performed by a light guide connected diode array spectrometer. The effective optical path length in the free beam was elongated by a multiple reflection system to about 0.9 m. The clusters were then deposited on  $\text{SiO}_2$  substrates or embedded by additional codeposition of  $\text{SiO}_2$  from an electron beam evaporation source. Cluster

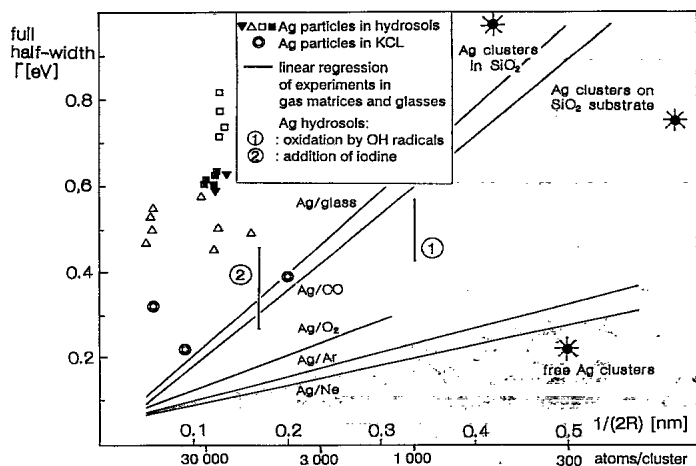


FIG. 3. Half-widths  $\Gamma$  of Mie extinction bands vs inverse cluster size, compiled for Ag clusters in various surroundings. Part of the figure stems from Ref. 6. The curves of Ag/CO, Ag/O<sub>2</sub>, Ag/Ar, Ag/Ne: Ref. 9; Ag/KCl: Ref. 41; Ag/glass: Ref. 7; Ag/hydrosols: see Ref. 6. The data for (1) and (2) were taken from Ref. 23. The three data points of the present experimental results are plotted as asterisks.

sizes and distributions were determined directly by TEM using carbon foils.

Our setup has the unique possibility to allow us *in situ* optical measurements of three different states of the Ag clusters produced within each run: (1) clusters in a free beam, (2) the same clusters deposited on SiO<sub>2</sub> substrates, and (3) the same clusters embedded in a SiO<sub>2</sub> matrix. Hence, the influences of different stabilization media could be determined with high accuracy.

### B. Results

Examples of recorded absorption spectra are shown in Figs. 4(a)–4(c). Spectra of three different runs are presented. They show the dipolar Mie absorption resonances for the above-described three different cluster environments. In Fig. 4(b), several spectra are plotted for increasing substrate coverage. The value of  $\Gamma$  plotted in Fig. 3 was chosen from the lowest coverage to avoid cluster-cluster interactions. In addition there is a strongly increasing tendency of the cluster to form larger coalescence aggregates if the coverage is increased. This becomes apparent in a redshift of the absorption bands and was confirmed by TEM analysis.

The spectra of Fig. 4(c), recorded for different volume densities (filling factors) of the clusters, are all similar to each other, i.e., they differ only by constant factors across the whole spectral region. This conclusively demonstrates that the clusters are well separated and noninteracting.

The indicated mean cluster sizes were determined from cubic averaging over individual diameters determined by TEM which is the apt way if Mie absorption is concerned. For comparison, also the linear average was

computed. For one sample where cubic averaging yielded  $2R = 2.0$  nm (300 atoms), the linear average amounted to 1.8 nm (200 atoms).

The drastic increases of bandwidth  $\Gamma_{\text{expt}}$  in Figs. 4(b) and 4(c) for supported and embedded clusters compared to Fig. 4(a) for the free clusters are striking. We attribute them to the presence of the media (here SiO<sub>2</sub>) partly or fully surrounding the clusters. In particular, we point to the extremely small width of the band of the free clusters. An abrupt jump upwards to a value  $A \approx 0.8$  is caused by depositing the clusters on the SiO<sub>2</sub> substrate. It is further raised to  $A \geq 1$  if the clusters are embedded in the SiO<sub>2</sub> matrix. Bandwidths of three spectra are plotted by an asterisk in Fig. 3. They were determined from the low-frequency flank of the Mie band only, because of the non-symmetric band shape in the case of Ag clusters.<sup>6</sup> Apparently, the  $\Gamma$  value of the free clusters is below the smallest value (the one of the Ne matrix) of all embedded samples. The corresponding  $A$  amounts to 0.25. Hence, very small  $\Gamma$  values combined with an extremely small size dependence  $\Gamma(R)$  are typical for free Ag clusters, i.e., clusters with free surfaces. Obviously, decay of the plasmon excitation (via energy, momentum, or phase dissipation) is less effective without the surrounding material.

For comparison, spectra computed from Mie's theory with the bulk Ag data of Johnson and Christy<sup>25</sup> which were cluster size corrected according to Eq. (8) are shown in Fig. 4(a). The two theoretical spectra differ in the choice of the  $A$  parameter. Clearly,  $A = 1$  gives a poor description, but the drastically reduced value  $A = 0.25$  reproduces the width of the measured spectrum. The peak position of the experiment (3.65 eV) differs from the one predicted by calculation (3.50 eV). The blueshift of

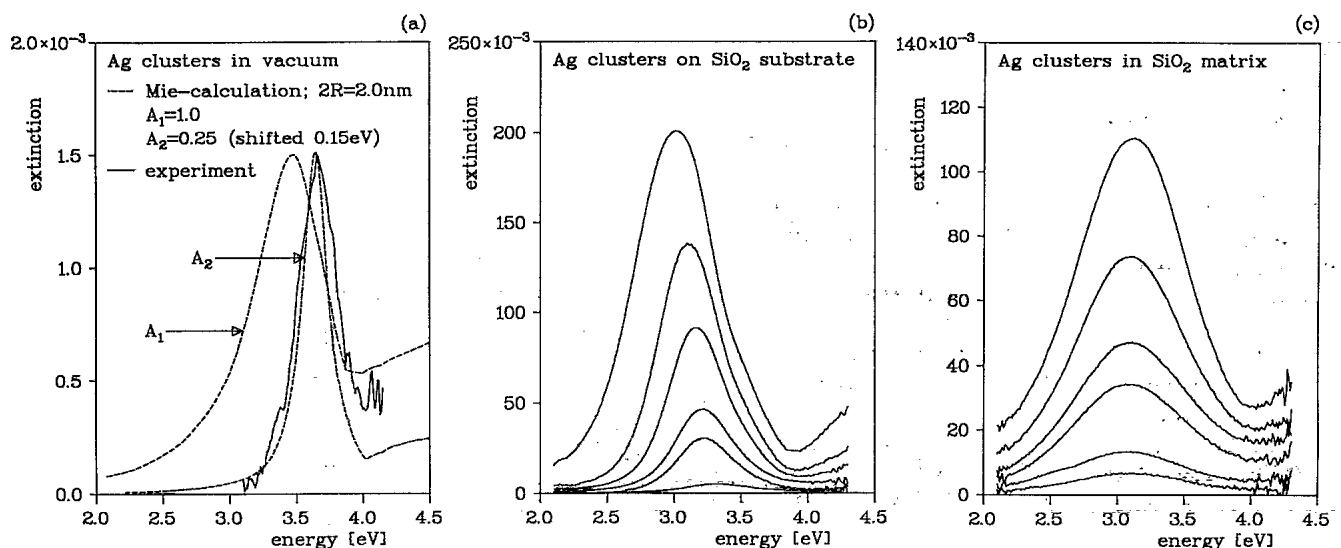


FIG. 4. Absorption spectra of Ag clusters produced as a free beam (see text). (a) Measured in the free beam and compared to Mie calculations performed with  $\epsilon(\omega)$  of (Ref. 25) after size correction by Eq. (8) using  $A = 1$  and  $A = 0.25$ , respectively. The curve for  $A = 0.25$  was shifted to the position of the measured spectrum in order to facilitate comparison. (b) Measured after deposition on a SiO<sub>2</sub>-glass substrate with different coverages increasing from bottom to top. (c) Measured after embedding in a coevaporated SiO<sub>2</sub> matrix with volume densities (filling factors) increasing from bottom to top. (Results of three different experimental runs with slightly different sizes are shown.) The peak positions are (a) 3.65 eV, (b) 3.30 eV (lowest curve), (c) 3.10 eV.

about 0.15 eV may be interpreted as due to the size dependence of the  $4d$ - $5sp$  interband transition edge which is expected to follow the narrowing of the  $4d$  band observed in ultraviolet photoemission spectroscopy studies.<sup>26</sup> It may thus be explained by size-dependent band structure and matrix elements [Eq. (7)]. Alternatively it could be produced by a size-dependent contraction of the Ag cluster surface which may be larger in free clusters than in embedded ones. As a consequence, the  $s$ -electron density  $n$  would be higher for free clusters, shifting the peak into the blue. This shift is into the opposite direction than would be expected from the  $s$ -electron spill-out effect of the free-electron metal.

The relative shift roughly corresponds to the experimental results of Ag clusters embedded in various weakly interacting matrices.<sup>9</sup> However, a quantitative comparison of  $A$  values deduced from Eq. (4) should be performed with care, since the peak positions depend on  $\epsilon_m$ , and  $d\epsilon_1/d\omega|_{\omega_1}$ , influencing  $\Gamma$  according to Eq. (10), varies with frequency  $\omega_1$ .

It is an interesting observation—also holding for the alkali metals—that the spectral position of the free plasmon peak almost coincides with the resonance lines of free atoms.

## VI. DISCUSSION

### A. Consequences for theoretical concepts

Quite probably deformations of the clusters towards oblate shapes occur during their impact on the substrate and to probably a smaller extent while being buried in the matrix. If statistically distributed these would give rise to an increased  $\Gamma$ . Still, however, the observed drastic changes cast doubt on presently accepted theories modeling  $\Gamma(R)$ . We will pick out two of them and reformulate them qualitatively in the light of the presented experimental results.

(1) The free path effect of Eq. (5) stems from the classical theory of conductivity and describes the limitation of the  $s$ -electron mean free path due to surface scattering. Various geometrical conditions have been treated<sup>7,10,27</sup> like the isotropic electron scattering ( $A=1$ ), the diffuse scattering ( $A=0.75$ ), and the additional limitation by internal grain boundaries ( $A>1$ ). Yet, details of the scattering process which was tacitly assumed to be inelastic concerning both momentum and energy increments were not discussed.

The alternative of specular (elastic) reflection of the electrons at the surface, which yields no size effect at all, was—to our knowledge—only treated in Ref. 28. The important consequence is the appearance of closed electron trajectories of various orders which have been connected to the shell structure. If this is the case for free clusters, i.e., if we assume no transfer of additional momentum and energy during the collision with the clean surface, then—within the frame of classical conductivity— $\Gamma$  should even remain independent of cluster size. In this case, only scattering at phonons, impurities, and defects within the cluster supplemented by electron-hole excitations in worse free-electron metals like Au or Cu, is responsible for the damping. It is then

the surrounding atoms or molecules which open an effective decay channel and thus induce the strong size dependencies  $\Gamma(R)$  observed experimentally in Fig. 4. How this decay could become operative will be discussed below in the context of the theory of Persson.<sup>13</sup>

Contributions of the free, uncovered surface to dissipation then depend on the amount of regular electron reflection expressed in the classical conductivity theory by the specularity parameter  $p$  of Fuchs and on the energy transfer from the electron cluster to the ion cluster via surface-enhanced electron-phonon interaction or recoil effect. The parameter may be included in Eq. (5) by replacing  $A$  with  $\Gamma A'(1-p)$ . Further, size-dependent densities of internal electron-scattering centers like grain boundaries<sup>27</sup> may contribute to the overall value of the experimentally determined  $A$ .

(2) The quantum-size effects (QSE) introduced by Kawabata and Kubo<sup>29</sup> and later repeatedly derived within different models<sup>8,30,31</sup> are based upon two assumptions: well-defined single quasiparticle states as in the potential box model and energetically separated by the confinement—thus being size dependent—and allowed direct electronic transitions between them which accomplish the dissipation of the plasmon energy. We mention that the resulting  $A$  parameters are between 0.3 and 3.<sup>6</sup>

Consequently, clusters with ideally smooth surfaces have  $A>0$  in contrast to the free path effect. Additional surface scattering as in (1) can be introduced via irregular box potentials.

In the case of the extremely high electron densities in good metals, the assumptions of the box model may not be adequate because strong electron interactions may broaden the excited states. This idea is supported by the up to now unsuccessful search for the corresponding discrete transitions by direct optical spectroscopy.

If, as in the potential box model the electron energy is purely kinetic, then single-electron transitions following the plasmon excitation may be regarded as causing dephasing of the collective motion, i.e., the coherent excitation is transferred into incoherent excitations of the internal degrees of freedom of the electron system (phase-coherence breaking). However, the mechanism of energy dissipation in a fully isolated cluster is not understood. The details of the energy and momentum transfer in the QSE towards the heat bath might be treated by box models, including a complex potential well.

Both of the above examples of models for the width, i.e., the damping  $\Gamma(R)$  of the collective electron resonances consider clusters with free surfaces. The influence of surrounding media was usually assumed to be of minor importance, i.e., just to be restricted to the influence of  $\epsilon_m$  in Eq. (1). Most experimental data from clusters in matrices have been compared to those theories developed for free clusters.

### B. Chemical interface damping

The presented experimental data corroborate the idea that the details of the cluster surface/interface are relevant and crucial beyond the influence of  $\epsilon_m$  in Eq. (1) of Mie's theory.<sup>10,13</sup> An example demonstrating the influence of surface roughness experimentally was given

in Fig. 4 of Ref. 6. There are several theories modeling the electron-photon coupling at electronic surfaces beyond the Maxwell boundary conditions of the Mie theory, which clearly demonstrate the influence of structural details of the free surface on the excitation of the Mie resonances.<sup>12,32</sup> The parameter  $A$ , derived in Ref. 12, depends on the frequency, on the Wigner-Seitz radius, and on the phenomenological Fuchs parameter  $p$ . For the free Ag cluster the numerical relation

$$\Gamma(R) = \Gamma_0 + [0.71 + (1-p)0.31] \frac{v_F}{R} \quad (11)$$

is obtained, which yields  $0.71 \leq A \leq 1.02$ . These values can neither explain the experimental result of  $A = 0.25$  for our free Ag clusters and the low  $A$  values obtained for those in rare-gas matrices (Fig. 3) nor can these theories explain the observed increase of the width for supported or embedded clusters.

We conclude from the results of Fig. 3 and 4 that the damping includes essential contributions of chemical interface damping (CID), that means it depends on the chemical properties of the interface and the energy transfer between cluster and surroundings by temporary charge-transfer reactions. This suggestion arose from the experiments of Charlé, Frank, and Schulze<sup>9</sup> and is on the one hand strongly supported by a recently developed theory of Persson<sup>13</sup> and on the other hand, there are close similarities to the interpretation of the chemical contribution to the surface-enhanced Raman-scattering effect by Otto.<sup>33</sup>

We assume the mechanism as follows. Upon colliding with the interface the excited electrons (which may be hot electrons of the plasmon excitation) are temporarily transferred into "affinity levels"<sup>33</sup> of the surrounding medium and back again. In this qualitative picture we do not stress the differences between an adsorbate and a surrounding compact medium. Residence times of the transferred electrons of the order of  $10^{-14}$  s are sufficient to disturb the phase coherence of the collective excitation. One important consequence of the electron transfer model of Persson is that the back transferred electrons have suffered inelastic scattering at the interface. Since the embedding matrix acts as an efficient heat bath, both momentum and energy increments of the transferred electrons can be dissipated, i.e., inelastic scattering of the electrons occurs. The  $(1/R)$  dependence is then the consequence of two effects: the number of  $s$  electrons, participating in the collective excitation is proportional to  $R^3$  whereas the number of adsorbate molecules is only proportional to  $R^2$ .

We assume that the plasmon excitation, which may be visualized by the oscillation of the Fermi sphere in  $k$  space, decays by cascades of individual scattering processes of all electrons involved in the excitation. Taking place, both successively and concurrently, within the plasmon decay time, they destroy the phase coherence and dissipate energy and momentum of the plasmon. Each electron can contribute likewise and the possible scattering mechanisms also involve the CID. The dynamics of the individual processes may be correlated and energy conservation must only hold cumulatively for

such cascades. As pointed out in Sec. II the excitation energies of the single electrons are very small compared to the plasmon energy. As a consequence, transitions close to  $E_F$  are important rendering a closer similarity to the case of electric conductivity than to optical excitations.

Since the single-electron excitation energies increase with decreasing cluster size (hot-electron effect), the electrons in very small clusters may be more effective in exciting adsorbate levels above the Fermi energy and hence, give rise to additional energy dissipation.

In principle, resonant CID occurs if the excitation energies at certain cluster sizes just coincide with adsorbate energy levels. In contrast to sharp atomic or molecular levels, adsorbate excitation states are extremely broadened and—for many substances—even extend down to the Fermi level of the clusters.<sup>13</sup> In this context the most important factor for the CID is the overlap of the adsorbate states with the occupied part of the cluster conduction band. The energy and width of the adsorbate states depend on the chemical character of the adsorbate and the cluster material, and this explains the widespread range of resulting  $A$  values.

This concept based upon the Persson theory therefore gives a physical explanation for the mechanism of the phase-coherence breaking and the energy and momentum dissipation into the heat bath of the surroundings. As this mechanism requires material around the cluster surface, smaller plasmon widths are expected for free clusters in full agreement with our observations. The CID enables effective inelastic processes and this explains why, e.g., the free path effect theory can successfully be applied to embedded clusters. The merit of Persson's theory is that the experimentally confirmed sensitivity of the slope constant  $A$  on the surrounding substances shown in Fig. 3 can now be traced back to the details of the involved adsorbate-induced affinity levels and thus they can, in principle, be calculated from a microscopic theory. In a first step, Persson was able to qualitatively explain the different  $A$  values obtained by Charlé, Frank, and Schulze<sup>9</sup> and by Ref. 7 for Ag clusters in various matrices. He also included a discussion of  $\text{SiO}_2$  as an embedding medium, which was used in our experiments.

### C. Comparison to recent work on alkali clusters

From Persson's model one expects still stronger CID for ligand stabilized metal-cluster compounds.<sup>34</sup> This is in agreement with the experimentally observed absence of even a hint for plasmon excitations in metal-organic  $\text{Au}_{55}$  clusters which, hence, may be due to extremely effective CID in addition to interband transition effects involving the  $5d$  electrons.<sup>29</sup>

Experimental results of the absorption of mass selected potassium and lithium cluster ions of similar sizes (140 to 1500 atoms) were recently obtained via an extension of beam depletion spectroscopy,<sup>35</sup> using a multiple photon absorption scheme.<sup>36</sup> Although this experiment is more complex than a direct transmission measurement, the results are compared in Fig. 5 with Mie absorption spectra computed with size corrected  $\epsilon$ . The results for the peak

shifts with respect to the Mie dipolar resonance calculated applying published  $\epsilon(\omega)$  of the bulk metals and the  $A$  parameters for the widths are compiled in Table I. Obviously these data are rather puzzling with respect to the present interpretation of the silver clusters. For both K and Li clusters, the resonances are redshifted whereas for Ag clusters they are blueshifted. The different shifts are among others due to the influences of  $d$  electrons which are strong in Ag. In K the  $s$ -electron spill-out and possibly also ion structure effects are predominant.

The bandwidths of the alkali clusters give rise to a number of questions. The two investigated potassium clusters have positive  $A$  values below unity (0.4 and 0.9) (optical functions from El Naby in Ref. 37) and are therefore compatible with the size-effect models although the  $A$  values are higher than expected from our results. In contrast the lithium clusters (optical functions of Ref. 38) have even smaller bandwidths than expected for bulk material, i.e., for  $A=0$ . Formally this would give rise to negative  $A$  values which makes no sense within the

TABLE I. Experimental widths,  $A$  parameters, and shifts of the resonance energies of potassium and lithium clusters from a comparison of experiment (Ref. 31) with Mie theory calculations using known dielectric functions (see text).

Clusters	Width (eV)	$A$ parameter	Shift of resonance energy $\Delta\tilde{\hbar}\omega$ (eV)
K <sub>500</sub> <sup>+</sup>	0.28	0.4	-0.24
K <sub>900</sub> <sup>+</sup>	0.40	0.9	-0.23
Li <sub>270</sub> <sup>+</sup>	1.15	<0	-0.5
Li <sub>440</sub> <sup>+</sup>	1.32	≈0	-0.5
Li <sub>820</sub> <sup>+</sup>	1.10	<0	-0.5
Li <sub>1500</sub> <sup>+</sup>	1.15	<0	-0.25

framework of the above models. Several arguments may be considered.

First, the experimental technique uses multiple absorption of photons. The clusters have high temperatures which may vary with size and the resulting rotations and shape fluctuations can give rise to particular damping mechanisms. The  $\epsilon(\omega)$  used in the present analysis were, yet, determined at room temperature.

Second, these optical material functions, to be inserted into the Mie theory, are crucial anyhow. As is well known, the situation is particularly obscure for the alkali metals, where several sets of incompatible data have been reported (see, e.g., Refs. 37 and 39). Hence, it might well be possible, that the used optical functions of lithium<sup>38</sup> are inadequate, i.e., do not resemble bulk material properties (it has been stressed in Ref. 38 that it is very difficult to obtain smooth clean thin films). In this case, even the  $A=0$  spectrum would already contain a contribution from roughness and film structure dependent  $\epsilon(\omega)$ , i.e., the true bulk values would be unknown. This problem cannot be controlled easily since lithium is also more difficult to treat theoretically than other alkali metals.

Third, the electronic behavior of lithium clusters may be basically different from that of bulk material, and then correct bulk optical functions—even if they were available—would not be applicable to calculate  $\epsilon(\omega, R)$ .

Fourth,  $\Gamma$  of Eq. (4) in fact includes two parameters,  $A$  and  $\Gamma_0$ . For the purpose of evaluating plots like Fig. 5(b) in terms of  $A$ ,  $\Gamma_0$  was assumed to be independent of  $R$  and follows from the bulk optical material functions by the extrapolation  $1/R \rightarrow 0$ . Alternatively, the experiments could be interpreted in terms of a size-dependent parameter  $\Gamma_0 = \Gamma_0(R)$  while—at the other extreme— $A$  is set to zero. A plausible motivation for such a procedure is that  $\Gamma_0$  is classically determined by collisions of the electrons with phonons, impurities, defects, etc. and by interband transitions. In small clusters, the concept of phonons loses its meaning; in addition one can imagine that depending on the nucleation conditions (growth velocity, temperature, etc.) the number of internal defects may vary and even strongly depend on size.<sup>27</sup>

In summarizing these arguments, the results for the lithium clusters with  $A < 0$  can presently not be understood from the Mie theory—extended to account for the

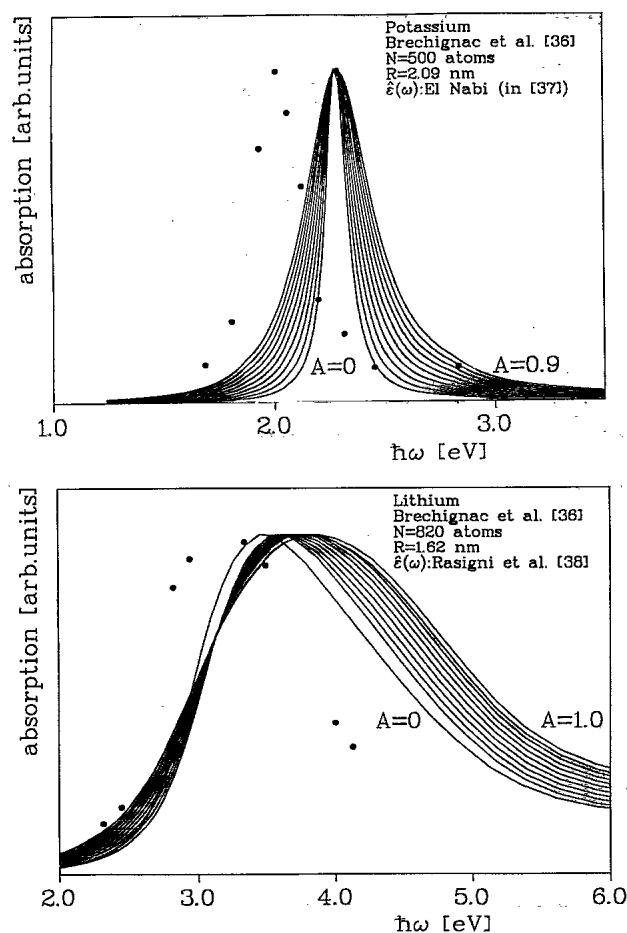


FIG. 5. Depletion spectra of size-selected free K and Li clusters measured by Bréchnagnac *et al.* (Ref. 36) (dots). They are compared to Mie absorption spectra which were calculated with bulk  $\epsilon(\omega)$  of Refs. 37 and 38, respectively, after size correction by Eq. (8). The slope parameter  $A$  was varied between  $A=0$  and  $A=1$ .

$1/R$  effect—by using the dielectric functions of Ref. 38 or similar ones [perhaps, it might be interesting to start from the other end and deduce  $\epsilon(\omega)$  by Kramers-Kronig analysis from the optical spectra of the clusters].

The Mie spectra of Li clearly indicate that this is not a good free-electron metal. In particular, an increase of the slope parameter  $A$ —which for K and Ag clusters gives rise to increased  $\Gamma$  while the peak position remains essentially unchanged—changes both width and peak positions for Li. The peak shifts in Table I of the Li clusters amount to 0.5 eV, twice as much as of the potassium clusters.

## VII. CONCLUSIONS

In conclusion, our direct optical spectroscopy experiments on neutral Ag clusters ( $2R \approx 2nm$ , i.e.,  $N \approx 300$ )—investigated alternatively in the free beam, on a substrate, and in a matrix—corroborate the existence and the importance of the chemical interface damping (CID) of Mie resonances in metal clusters. Hence, detailed microscopic calculations for  $A$  parameters are desirable for a quantitative comparison with the experimental results. In free clusters, the resonance lifetime appears to be drastically increased due to the lack of this dissipation channel. On the other hand, CID is expected to be particularly strong, if the interfaces are formed by chemisorbed material, by material with high ionicity (as, e.g., in the cases of aqueous electrolyte solvents and halide crystal matrices) or by chemically bound ligands. Qualitatively this is confirmed by the experimental results in Fig. 3. It is, however, still unclear why the width in these

cases does not follow Eq. (4). Rather a large and size-independent contribution  $\Gamma_0$  dominates depending on chemical details like charge-transfer reactions, etc. which can easily conceal present size dependencies. It is a fascinating idea to use these effects for monitoring chemical surface reactions.<sup>23</sup>

Kawabata and Kubo<sup>29</sup> stated that the cluster surface determines the electronic eigenstates rather than to act as a scatterer. In light of the present discussion this statement holds for free clusters but not for supported or embedded clusters where surface scattering due to CID becomes effective. Obviously cluster-size-effect theories which describe the experimentally observed Mie resonance bands in cluster matter have to consider the details of the energy and momentum transfer and phase breaking, the most prominent effect probably being CID, if adsorbates, substrates, or matrices are present.

In conclusion, the  $(1/R)$  law appears not to be universal<sup>40</sup> concerning the electron dynamics in metal clusters, since the slope constant  $A$  proves to depend sensitively on preparation details and properties of the regarded cluster system. It is quite a different and still open question of how this plasmon behavior merges into the distinct and narrow spectral lines of very small molecules and finally the atom.

## ACKNOWLEDGMENT

We are indebted to the Deutsche Forschungsgemeinschaft for financial support.

- <sup>1</sup>V. Bonacic-Koutecky, P. Fantucci, and J. Koutecky, *Chem. Rev.* **91**, 1035 (1991).
- <sup>2</sup>W. Ekardt, *Phys. Rev. Lett.* **52**, 1925 (1984); *Phys. Rev. B* **31**, 6360 (1985).
- <sup>3</sup>U. Kreibig and P. Zacharias, *Z. Phys.* **231**, 128 (1970).
- <sup>4</sup>M. Vollmer and U. Kreibig, in *Nuclear Physics Concepts in the Study of Atomic Cluster Physics*, edited by R. Schmidt, H. O. Lutz, and R. Dreizler, *Lecture Notes in Physics Vol. 404* (Springer, Berlin, 1992), p. 266.
- <sup>5</sup>T. Hollstein, U. Kreibig, and F. Leis, *Phys. Status Solidi B* **82**, 545 (1977).
- <sup>6</sup>U. Kreibig and L. Genzel, *Surf. Sci.* **156**, 678 (1985).
- <sup>7</sup>U. Kreibig and C. v. Fragstein, *Z. Phys.* **224**, 307 (1969); U. Kreibig, *J. Phys. F* **4**, 999 (1974).
- <sup>8</sup>L. Genzel, T. P. Martin, and U. Kreibig, *Z. Phys. B* **21**, 339 (1975).
- <sup>9</sup>K.-P. Charlé, F. Frank, and W. Schulze, *Ber. Bunsenges. Phys. Chem.* **88**, 350 (1984).
- <sup>10</sup>M. Vollmer and U. Kreibig, *Optical Properties of Metal Clusters*, Springer Series in Material Science (Springer, Berlin, in Press).
- <sup>11</sup>U. Kreibig, *Z. Phys.* **234**, 307 (1970); *J. Phys.* **38**, C2-97 (1977).
- <sup>12</sup>P. Apell, R. Monreal, and F. Flores, *Solid State Commun.* **52**, 971 (1984); P. Apell and D. R. Penn, *Phys. Rev. Lett.* **50**, 1316 (1983).
- <sup>13</sup>B. N. J. Persson, *Surf. Sci.* **281**, 153 (1993).
- <sup>14</sup>F. Bassani and G. Pastori Parravicini, *Electronic States and Optical Transitions in Solids* (Pergamon, New York, 1975).
- <sup>15</sup>U. Kreibig, K. Fauth, C. G. Granqvist, and G. Schmid, *Z. Phys. Chem. (Ber. Bunsenges.) Nene Folge* **169**, 11 (1990).
- <sup>16</sup>U. Kreibig, *Appl. Phys.* **10**, 255 (1976).
- <sup>17</sup>D. M. Mann and H. P. Broida, *J. Appl. Phys.* **44**, 4950 (1973); J. D. Eversole and H. P. Broida, *Phys. Rev. B* **15**, 1644 (1977); J. Hecht, *J. Opt. Soc. Am.* **70**, 694 (1980).
- <sup>18</sup>S. Mochizuki and R. Ruppig, *J. Phys. Condens. Matter* **5**, 135 (1993).
- <sup>19</sup>A. H. Pfund, *Rev. Sci. Instrum.* **1**, 397 (1930).
- <sup>20</sup>K. Rademann, O. Dimopoulou-Rademann, M. Schlauf, U. Even, and F. Hensel, *Phys. Rev. Lett.* **69**, 3208 (1992).
- <sup>21</sup>H. Haberland, B. v. Issendorff, J. Yufeng, and T. Kolar, *Phys. Rev. Lett.* **69**, 3212 (1992).
- <sup>22</sup>R. Zsigmondy, *Kolloidchemie* (Spamer, Leipzig, 1927).
- <sup>23</sup>A. Henglein, *Chem. Rev.* **89**, 1861 (1989); A. Henglein, P. Mulvaney, and T. Linnert, *Farad. Disc.* **92**, 31 (1991); T. Linnert, P. Mulvaney, and A. Henglein, *J. Phys. Chem.* **97**, 679 (1993).
- <sup>24</sup>O. F. Hagen, *Z. Phys. D* **20**, 425 (1991); O. F. Hagen, G. Knop, and G. Linker, in *Physics and Chemistry of Finite Systems: From Clusters to Crystals*, Vol. II of *NATO Advanced Study Institute Series C: 374*, edited by P. Jena, S. Khanna, and B. Rao (Kluwer, Dordrecht, 1992), p. 1233.
- <sup>25</sup>P. B. Johnson and R. W. Christy, *Phys. Rev. B* **6**, 4370 (1972).
- <sup>26</sup>R. Baetzold, *J. Am. Chem. Soc.* **103**, 6116 (1981).
- <sup>27</sup>U. Kreibig, *Z. Phys. B* **31**, 39 (1978).
- <sup>28</sup>R. Balian and C. Bloch, *Ann. Phys. (N.Y.)* **69**, 76 (1972).
- <sup>29</sup>A. Kawabata and R. Kubo, *J. Phys. Soc. Jpn.* **21**, 1765 (1966).
- <sup>30</sup>R. Ruppig and H. Yatom, *Phys. Status Solidi B* **74**, 647 (1976).
- <sup>31</sup>C. Yannouleas and R. A. Broglia, *Ann. Phys. (N.Y.)* **217**, 105

- (1992).
- <sup>32</sup>A. Liebsch, *Phys. Rev. B* **40**, 3421 (1989).
- <sup>33</sup>A. Otto, *J. Raman Spectrosc.* **22**, 743 (1992).
- <sup>34</sup>G. Schmid, *Structure and Bonding* **62**, 51 (1985); *Polyhedron* **7**, 2321 (1988).
- <sup>35</sup>W. A. de Heer, K. Selby, V. Kresin, J. Masui, M. Vollmer, A. Châtelain, and W. D. Knight, *Phys. Rev. Lett.* **59**, 1805 (1987); K. Selby, M. Vollmer, J. Masui, V. Kresin, W. A. de Heer, and W. D. Knight, *Phys. Rev. B* **40**, 5417 (1989).
- <sup>36</sup>C. Bréchnignac, Ph. Cahuzac, N. Kebaïli, J. Leygnier, and A. Sarfati, *Phys. Rev. Lett.* **68**, 3916 (1992); C. Bréchnignac, Ph. Cahuzac, J. Leygnier, and A. Sarfati, *Phys. Rev. Lett.* **70**, 2036 (1993).
- <sup>37</sup>M. H. El Naby, *Z. Phys.* **174**, 269 (1963).
- <sup>38</sup>M. Rasigni and G. Rasigni, *J. Opt. Soc. Am.* **67**, 54 (1977).
- <sup>39</sup>T. Inagaki, L. C. Emerson, E. T. Arakawa, and M. W. Williams, *Phys. Rev. B* **13**, 2305 (1976), and references therein.
- <sup>40</sup>J. Jortner, *Z. Phys. D* **24**, 247 (1992).
- <sup>41</sup>S. Jain and N. Arora, *J. Phys. Chem. Solids* **35**, 1231 (1974).